TPR-96-19

Feynman rules in radial gauge

S. Leupold
Institut für Theoretische Physik, Universität Regensburg,
D-93040 Regensburg, Germany
and
Institut für Theoretische Physik, Justus-Liebig-Universität Giessen,
D-35392 Giessen, Germany
(September 26, 1996)

Abstract

We present a complete set of Feynman rules for non-Abelian gauge fields obeying the radial (Fock-Schwinger) gauge condition and prove the consistency with covariant gauge Feynman rules.

11.15Bt,12.38Bx

I. INTRODUCTION

Perturbation theory for non-Abelian gauge fields is usually formulated in covariant gauges. There the Feynman rules nearly can be read off from the momentum space representation of the Lagrange density including gauge fixing and Faddeev-Popov ghost terms (c.f. any textbook on gauge field theory, e.g. [1]). The only subtlety is the proper pole prescription for the propagator $1/k^2$ which is achieved by the causal ϵ prescription, i.e. by the physically motivated requirement that particles (antiparticles) propagate forward (backward) in time.

Despite the great success of covariant gauge Feynman rules there are situations where a different gauge choice is preferable. However it turned out during the last 15 years that things are much more involved if perturbation theory ought to be formulated in non-covariant gauges. The most prominent example is the case of temporal gauge where an additional pole $(1/k_0^2)$ appears in the gauge field propagator. Assuming the absence of ghost contributions and temporal propagator modes it was shown first in [2] that the actual value of gauge invariant quantities depends on the pole prescription for this additional propagator pole (see also [3] and references therein). According to [4] this pole is caused by the fact that the temporal gauge condition is insufficient to completely fix the gauge degrees of freedom. A complete gauge fixing condition, on the other hand, automatically regulates this "gauge pole", albeit breaks translational [4] or rotational [5] invariance, which at least makes the use of temporal gauge Feynman rules less attractive.

A second example is the Coulomb gauge where singularities appear in the energy integrations of two loop diagrams [6–9]. These singularities must be cured by a very subtle prescription [8,9] or alternatively by the introduction of new multi-gluon vertices [10]. As already pointed out in [10] these problems are due to operator ordering ambiguities which are difficult to handle in the path integral approach.

These examples show that it is far from being trivial to find consistent sets of Feynman rules for non-covariant gauges. With "consistent" we simply mean that a given set of Feynman rules reproduces the same value for any gauge invariant quantity as the covariant gauge Feynman rules. The consistency of different sets of momentum space Feynman rules was systematically studied by Cheng and Tsai [6,7,11]. A diagrammatic scheme was developed in [6,11] which serves to prove without analytic calculations that different sets of Feynman rules yield the same results for gauge invariant quantities. Cheng and Tsai called this the "theorem of equivalence". To apply this scheme to a given set of Feynman rules the propagators must not have any singularity, i.e. every singularity must be regulated and the regulator must be kept finite during the course of calculation. E.g. for the case of temporal gauge it was shown [7] that some prescriptions of the gauge pole mentioned above reintroduce ghost fields and/or temporal propagator modes which vanish if the regulator is taken to zero but nevertheless contribute to loop integrals as long as the regulator is kept finite. Hence the discrepancy between covariant and temporal gauge calculations observed in [2] is due to the neglect of ghost and temporal propagator modes in the temporal gauge using a specific gauge pole prescription, namely the principal value prescription.

In this article we will present a set of Feynman rules for the radial (Fock-Schwinger) gauge and apply the diagrammatic scheme of Cheng and Tsai to this set of rules to show its consistency with covariant gauge Feynman rules. The radial gauge with its gauge condition

$$x_\mu A^\mu(x) = 0 \tag{1.1}$$

was introduced long time ago [12,13] and rediscovered several times (e.g. [14]). It found widespread use in the context of QCD sum-rules (e.g. [15]) since it enormously simplifies the task of organizing the operator product expansion of QCD n-point functions in terms of gauge invariant quantities by expressing the gauge potential via the gauge covariant field strength tensor.

In (1.1) the origin is singled out by the gauge condition. Therefore this gauge condition breaks translational invariance and perturbation theory cannot be formulated in momentum space as usual but must be set up in coordinate space. For this reason only few efforts have been made to establish perturbation theory for radial gauge [16–21]. Most of the discussion was concentrated on the question about the properties of the free radial gauge propagator while less efforts where made to explore the other Feynman rules, especially to figure out if ghost fields truly decouple. Recently a radial propagator with surprising properties was proposed in [21].

In the next Section we briefly recapitulate the results found in [21]. In Sec. III we generalize the diagrammatic scheme of Cheng and Tsai, originally developed for momentum space, to coordinate space Feynman rules. In Sec. IV we apply this scheme to a complete set of radial gauge Feynman rules including the radial gauge field propagator proposed in [21]. An additional check for the consistency of this set is presented in Sec. V using the Slavnov-Taylor identities of radial gauge. Finally we summarize our results in Sec. VI.

II. THE RADIAL GAUGE PROPAGATOR

In the following we work in a D-dimensional Minkowski space, i.e. with one time and $D-1$ space dimensions.

In [21] it was shown that the (full) radial gauge field propagator can be expressed in terms of a gauge invariant Wilson loop in the following way:

$$D^{ab}_{\mu\nu}(x,y) := \langle A^a_\mu(x) A^b_\nu(y)\rangle = \delta^{ab}\frac{2N}{N^2-1}\frac{1}{(ig)^2}\lim_{\substack{x'\to x\\ y'\to y}} \partial^x_\mu \partial^y_\nu\, W_1(x,x',y,y')\,. \tag{2.1}$$

where N is the numbers of colors and the Wilson loop W_1 connects the sequence of points $0, y', y, 0, x', x, 0$ along straight lines (c.f. Fig. 1). As a Wilson loop with cusps and self-intersections W_1 has so-called "cusp singularities" (c.f. [22] and references therein) appearing at quadratic (and higher) order in the coupling constant. Due to the prefactor $1/g^2$ in (2.1) these singularities show up at order g^0, i.e. already for the free radial propagator. The explicit form of the latter is given by

$$\begin{aligned}
&\langle A^a_\mu(x) A^b_\nu(y)\rangle_0 = \\
&= \frac{\Gamma(D/2-1)}{4\pi^{D/2}}\,\delta^{ab}\Big(g_{\mu\nu}[(x-y)^2-i\epsilon]^{1-D/2} \\
&\qquad - \partial^x_\mu \int_0^1 ds\, x_\nu\,[(sx-y)^2-i\epsilon]^{1-D/2} - \partial^y_\nu \int_0^1 dt\, y_\mu\,[(x-ty)^2-i\epsilon]^{1-D/2}
\end{aligned}$$

$$+\,\partial_\mu^x\partial_\nu^y \underbrace{\int_0^1 ds \int_0^1 dt\, x\cdot y\,[(sx-ty)^2-i\epsilon]^{1-D/2}}_{\sim \frac{1}{4-D}}\Big)\,. \tag{2.2}$$

which is obviously singular for $D \to 4$. That the free radial propagator diverges in four dimensional space was already pointed out earlier in [17]. The reason for this singularity was presented in [21]. It is a surprising result that the renormalization properties of a special class of Wilson loops influence even the free radial propagator. However it was argued in [21] that this singularity is even necessary to reproduce correct results for gauge invariant quantities calculated in radial gauge.

Note that we have used dimensional regularization for convenience. Of course the cusp singularities of Wilson loops and therefore also the singularity of the radial propagator might be regularized in a different way as well. In any case the regulator has to be kept finite during the calculation which however is required for loop calculations anyway. In addition a finite regulator is necessary to make the diagrammatic scheme of Cheng and Tsai applicable to radial gauge Feynman rules.

III. THE THEOREM OF EQUIVALENCE IN COORDINATE SPACE

The theorem of equivalence was originally formulated by Cheng and Tsai for momentum space Feynman rules [6]. In this section we generalize it to coordinate space. The basic statement is that all gauge invariant quantities are independent of the arbitrary function $\Delta_\mu(x,y)$ if the following Feynman rules are used:
The free gauge field propagator

$$D^{ab}_{\mu\nu}(x,y) = \delta^{ab}\left[D^F_{\mu\nu}(x,y) - \partial^x_\mu\,\Delta_\nu(x,y) - \partial^y_\nu\,\Delta_\mu(y,x)\right]\,, \tag{3.1}$$

the ghost field

$$G^{abc}_\mu(y,x) = -igf^{abc}\left[(g_{\mu\nu}\Box_x - \partial^x_\mu\partial^x_\nu)\Delta^\nu(y,x) + \partial^\nu_y\,D^F_{\mu\nu}(x,y)\right]\,, \tag{3.2}$$

and the common three and four gluon vertices. Here $D^F_{\mu\nu}$ denotes the Feynman propagator given in Appendix A, the "ghost field" is the product of ghost-gluon vertex and ghost propagator, and the coordinate space representation of the three and four gluon vertices is also given in Appendix A. Note that we get the expressions for Feynman gauge for vanishing Δ_μ. Hence the ghost field (3.2) can be written as

$$G^{abc}_\mu(y,x) = -igf^{abc}(g_{\mu\nu}\Box_x - \partial^x_\mu\partial^x_\nu)\Delta^\nu(y,x) + G^{F\,abc}_\mu(y,x)\,. \tag{3.3}$$

To prove that all gauge invariant quantities are independent of Δ_μ we observe that in the expression for the gauge propagator (3.1) Δ_μ is always accompanied by a partial derivative. This reflects the fact that the gauge modes and the longitudinal modes coincide in the free field case of a gauge theory. By partial integration we arrive at an expression where this partial derivative acts on a vertex which is connected to the propagator. The partial derivative acts on a three gluon vertex (A4) as

$$\partial_w^\lambda T^{abc}_{\lambda\mu\nu}(w,x,y) = igf^{abc}\Big[\delta(w-y)(g_{\nu\mu}\Box_w - \partial_\nu^w\partial_\mu^w)\delta(w-x) - \delta(w-x)(g_{\mu\nu}\Box_w - \partial_\mu^w\partial_\nu^w)\delta(w-y)\Big]\,. \tag{3.4}$$

Obviously the operators inside the brackets project on transverse components, i.e.

$$(g_{\nu\mu}\Box_w - \partial_\nu^w\partial_\mu^w)\partial_w^\mu = 0\,. \tag{3.5}$$

These operators act on the next propagator which is connected to the vertex at x,μ,b or y,ν,c, respectively, e.g.

$$\begin{aligned} &igf^{abc}\int d^Dx\,(g_{\nu\mu}\Box_w - \partial_\nu^w\partial_\mu^w)\delta(w-x)D^{\mu\mu'}_{bb'}(x,x') \\ &= -gf^{ab'c}g_\nu{}^{\mu'}\delta(w-x') + \partial_{x'}^{\mu'}\,G_\nu^{ab'c}(x',w)\,. \end{aligned} \tag{3.6}$$

This yields ghost type structures as well as contractions $-gf_{ab'c}g_\nu{}^{\mu'}\delta(w-x')$. As we shall show in the following the former cancel gauge dependent contributions from ghost loops while the latter are related to four gluon vertices. From (3.4) and (3.6) we get

$$\begin{aligned} &\int d^Dx\,d^D\,y\,\partial_w^\lambda\,T^{abc}_{\lambda\mu\nu}(w,x,y)D^{\mu\mu'}_{bb'}(x,x')D^{\nu\nu'}_{cc'}(y,y') = \\ &\int d^Dy\left[-gf^{ab'c}g_\nu{}^{\mu'}\delta(w-x')\,\delta(w-y) + \partial_{x'}^{\mu'}\,G_\nu^{ab'c}(x',w)\,\delta(w-y)\right]D^{\nu\nu'}_{cc'}(y,y') \\ &-\int d^Dx\left[-gf^{abc'}g_\mu{}^{\nu'}\delta(w-y')\,\delta(w-x) + \partial_{y'}^{\nu'}\,G_\nu^{abc'}(y',w)\,\delta(w-x)\right]D^{\mu\mu'}_{bb'}(x,x')\,. \end{aligned} \tag{3.7}$$

So far this looks very complicated. However a graphical representation of this formula is rather simple and indeed all calculations which are necessary to prove the theorem of equivalence can be performed graphically. Once all rules are stated, there is no need to write down any analytical expression. Formula (3.7) is depicted in Fig. 2. In the following all lines labeled with D denote gluon propagators. Three and four gluon vertices are dotted. G denotes a ghost field which includes a vertex and a propagator line according to the definition (3.2). An arrow at the end of a propagator line denotes a partial derivative acting on the respective vertex. Finally an arrow appearing as a label denotes the contraction mentioned above, i.e. the first contribution on the r.h.s. of (3.6).

Instead of presenting a complete set of diagrammatic rules first and applying it to an example afterwards we will choose a simple example right now and introduce the necessary rules step by step as soon as we need them. As an example we take the two loop vacuum contributions shown in Fig. 3. The combinatorial factors for these diagrams are 1/12 for the diagram involving three gluon vertices, 1/8 for the four gluon vertex diagram and 1/2 for the diagram with a ghost loop. It is useful to state the relative statistical weights and signs of all diagrams explicitly. This is depicted in Fig. 4. An overall factor 1/12 is suppressed. In addition the diagrams are symmetrized with respect to the propagator lines.

To prove the gauge invariance of the sum shown in Fig. 4 we have to show that the result remains the same if all D's and G's are replaced by D^F and G^F, respectively. To do that we will even prove a somewhat more rigorous statement: The sum remains the same if all fields D and G labeled by the same number are changed to D^F and G^F no matter of the gauge of the fields with different numbers. Thus we will prove in the following that without changing

the actual value of the whole sum D_1 and G_1 can be replaced by D_1^F and G_1^F without any reference to the explicit form of $D_{2,3}$ and $G_{2,3}$. This is enough to prove gauge invariance since this scheme can be applied to the diagrams of Fig. 4 consecutively for three times: In the first step D_1 and G_1 are changed to D_1^F and G_1^F. Next D_2 and G_2 can be replaced by D_2^F and G_2^F in the same way now dealing with D_1^F, G_1^F, D_3, and G_3. Finally D_3 and G_3 are replaced by their Feynman gauge expressions starting from diagrams where the lines labeled by 1 and 2 already are in Feynman gauge. Thus we will prove that the gauge of *one* line in *all* diagrams can be changed without changing the value of the sum of diagrams.

We start with the first diagram of Fig. 4 and decompose D_1 in its Feynman and Δ parts according to (3.1). This is shown in Fig. 5 where a partial integration has already been performed changing the relative sign of the Δ contributions with respect to the Feynman part.

Now we use the diagrammatic rule of Fig. 2 to obtain Fig. 6.

In this way we get two types of diagrams. The first type involves ghosts and partial derivatives (arrows). The latter act on the second three gluon vertex and we can use (3.4) again. In addition to (3.6) we need a relation where the propagator D is replaced by Δ. However this is nothing but (3.3). Using (3.4), (3.6) and (3.3) we get

$$\begin{aligned}
&\int d^Dx\, d^Dy\, \partial_w^\lambda\, T^{abc}_{\lambda\mu\nu}(w,x,y)\Delta^\mu(x',x)D^{\nu\nu'}_{cc'}(y,y') = \\
&\int d^Dy \left[G^{F\,abc}_\nu(x',w)\,\delta(w-y) - G^{abc}_\nu(x',w)\,\delta(w-y)\right] D^{\nu\nu'}_{cc'}(y,y') \\
&- \int d^Dx \left[-g f^{abc'} g_\mu{}^{\nu'}\,\delta(w-y')\,\delta(w-x) + \partial^{\nu'}_{y'}\, G^{abc'}_\mu(y',w)\,\delta(w-x)\right]\Delta^\mu(x',x)
\end{aligned} \tag{3.8}$$

which is shown in Fig. 7.

For a diagram of Fig. 6 with a ghost line we get Fig. 8. As a first example how the cancelation of gauge dependent diagrams shows up we note that the second diagram on the r.h.s. of Fig. 8 is identical to diagram G of Fig. 4. These diagrams cancel each other (note the minus sign in front of the third diagram of Fig. 6).

The last diagram of Fig. 8 can be transformed in a diagram with a ghost loop in the following way: The action of the arrow (partial derivative) on the ghost vertex can be split up in a sum of two terms using the product rule of differentiation.[1] On the one hand the partial derivative acts on a ghost field as (cf. (3.3))

$$\partial^x_\mu G^\mu_{abc}(y,x) = \partial^x_\mu G^\mu_{F\,abc}(y,x) = -g f_{abc}\delta(x-y)\,, \tag{3.9}$$

and on the other hand it acts on the upper line. This is shown in Fig. 9. The corresponding equation is

$$\begin{aligned}
&\int d^Dx\,\delta(v-x)\,\partial^x_\mu\left[G^\mu_{abc}(y,x)\,\delta(x-w)\right] = \\
&- \int d^Dx\,\delta(x-w)\,\partial^x_\mu\left[G^\mu_{abc}(y,x)\,\delta(v-x)\right] - \int d^Dx\,\delta(v-x)\,g f_{abc}\delta(x-y)\,\delta(x-w)
\end{aligned} \tag{3.10}$$

---

[1] It is interesting to mention that the momentum space equivalent of this product rule is the energy-momentum conservation at the vertex.

and the symbol **1** in Fig. 9 denotes the last integrand.

In this way the last diagram of Fig. 8 yields two new diagrams as shown in Fig. 10. Since the only difference between **1** and the contraction arrow is a $g_{\mu\nu}$-term it is easy to get the last line of Fig. 10.

Now we collect all diagrams which can be deduced from the two diagrams involving G's shown in Fig. 6 and compare the result, Fig. 11, with the original diagrams of Fig. 4: In addition to the ten diagrams of Fig. 11 we get ten analogous diagrams not shown here from the last diagram of Fig. 5. We refer to these diagrams as the "reflected" diagrams of the ones shown in Fig. 11. Diagrams a and b of Fig. 11 replace G_1 by G_1^F in Fig. 4G. The same is achieved by f and g in Fig. 4I. The corresponding reflected diagrams transform Fig. 4F and J in the same way. Diagrams c and j as well as e and h cancel each other. Diagram d and the reflected diagram of i replace D_1 by D_1^F in Fig. 4H. In the same way Fig. 4E is transformed by Fig. 11i and the reflected diagram of Fig. 11d.

Thus for the diagrams E-J of Fig. 4 we have already succeeded in replacing D_1 and G_1 by D_1^F and G_1^F. We are left with the four gluon vertex diagrams B and C on the one hand[2] and with the ghost-free diagrams of Fig. 6 and their reflected diagrams on the other hand. In Fig. 12 we have decomposed D_1 of Fig. 4B using (3.1).

Obviously we need a relation which connects contraction arrows with four gluon vertices. Indeed the following relation holds

$$\begin{aligned}
&-\int d^D w'\, g f_{abe} g^{\lambda}{}_{\lambda'} \delta(v-w)\,\delta(v-w')\, T^{\lambda'\mu\nu}_{ecd}(w',x,y) \\
&+\int d^D x'\, g f_{aec} g^{\mu}{}_{\mu'} \delta(v-x)\,\delta(v-x')\, T^{\mu'\nu\lambda}_{edb}(x',y,w) \\
&+\int d^D y'\, g f_{aed} g^{\nu}{}_{\nu'} \delta(v-y)\,\delta(v-y')\, T^{\nu'\lambda\mu}_{ebc}(y',w,x) = \partial^v_\kappa Q^{\kappa\lambda\mu\nu}_{abcd}(v,w,x,y)\,. \qquad (3.11)
\end{aligned}$$

This is shown in Fig. 13. Connecting the upper legs with each other and also the lower legs we find that the last but one diagram of Fig. 6 and its reflected diagram exactly cancel the last diagram of Fig. 12.[3] The same holds true for the diagrams where D_2 is replaced by D_3, i.e. Fig. 4C instead of B and the second diagram of Fig. 6 instead of the fourth.

We conclude that the last two diagrams of Fig. 5 can be decomposed in a way that the resulting diagrams can be used to replace D_1 and G_1 by D_1^F and G_1^F in Fig. 4B-J. This proves the theorem of equivalence for our example of two loop vacuum bubbles.

In the same way the theorem of equivalence can be proven for higher loop vacuum diagrams, scattering amplitudes and Wilson loops. There are a few more diagrammatic rules collected in Appendix B which we did not need here for our explicit example. However they become important for higher order Feynman diagrams. The complete set of diagrammatic rules, Figs. 2, 7, 9, 13, 15, 16, and 17, can be applied to any gauge invariant quantity in any order of the coupling constant. The necessary steps to prove the gauge invariance of a sum of loop diagrams are as follows:

---

[2]Diagram D remains unchanged since no D_1 appears there.

[3]Note that the third diagram of Fig. 13 vanishes due to its color structure if the upper legs are connected.

- Symmetrize all diagrams with respect to all lines (as shown in Fig. 4).
- Start with the diagrams which have only three-gluon vertices. Decompose one gluon propagator according to (3.1).
- Use Fig. 2 and 7 as long as there are ∂_μ-arrows pointing at a three-gluon vertex.
- Use Fig. 9 to pull arrows out of closed ghost loops (c.f. Fig. 10).
- At this stage all Δ_μ-dependent diagrams which have neither contraction arrows nor four-point vertices should drop out.
- Finally, diagrams with different topology are related by the rules of Figs. 13, 15, 16. To get an idea which diagrams are related it is instructive to contract the lines with contraction arrows.
- For Wilson loops the additional relation shown in Fig. 17 has to be taken into account.

This scheme can also be generalized to cases where the Yang-Mills fields are coupled to matter fields. In principle for each new vertex two new diagrammatic rules must be found, which have to show how the two introduced arrows (denoting the partial derivative and the contraction) act on this new vertex. For the case of full QCD (albeit using momentum space Feynman rules) this complete set of diagrammatic rules is given in [23] and applied to three loop diagrams. Independently of the original work of Cheng and Tsai [6] a similar set of diagrammatic rules was developed recently by Feng and Lam also for momentum space Feynman rules and applied to QCD [24] and electro-weak theory [25] to simplify perturbative calculations by choosing an appropriate gauge.

With the diagrammatic scheme developed in this Section we return to the case of radial gauge Feynman rules.

IV. APPLICATION TO RADIAL GAUGE

Now we have developed all tools necessary to present a consistent set of radial gauge Feynman rules. The free radial gauge field propagator is given in (2.2). To make the scheme of Cheng and Tsai applicable the regulator (here $D-4$) has to be kept finite until the end of the calculation. Note however that the regularized propagator already fulfills the radial gauge condition. This is in contrast to the case of temporal gauge. There the temporal mode of the propagator vanishes only if the regulator vanishes. This mode, however, couples to the ghost fields. As we shall see in the following ghost fields decouple for radial gauge since already the regularized propagator strictly satisfies the gauge condition.

Comparing (3.1) with (2.2) we get

$$\Delta_\nu(x,y) = x^\alpha \int_0^1 ds\, D^F_{\alpha\nu}(sx,y) - \frac{1}{2}\partial_y^\alpha \int_0^1 ds \int_0^1 dt\, x\cdot y\, D^F_{\alpha\nu}(sx,ty)\,. \tag{4.1}$$

After some simple algebraic manipulations we find that according to (3.2) the appropriate ghost field is given by

$$G^{abc}_{\nu}(x,y) = -igf^{abc}\left[x_\nu \int\limits_0^1 ds\,\delta(sx-y) - \partial^\alpha_y\, D^F_{\alpha\nu}(0,y)\right]. \tag{4.2}$$

It is easy to see that

$$G^{abc}_{\nu}(x,y) \sim y_\nu \tag{4.3}$$

holds. On account of the gauge condition (1.1) we find

$$G^{abc}_{\nu}(x,y) D^{\nu\nu'}_{cc'}(y,y') = 0\,. \tag{4.4}$$

Thus the ghost fields decouple from the gauge fields. Of course one expects that to happen for gauge fields obeying an algebraic gauge condition. As mentioned in the introduction this is however a non-trivial problem for the case of temporal gauge. This example teaches us that it is not sufficient to simply study the Faddeev-Popov ghost determinant. A more careful examination, e.g. like the one presented here, is necessary to state the decoupling of ghost fields.

One subtlety has to be clarified before we can apply the scheme developed in the last Section to our case at hand: One frequently used tool for the manipulations of Feynman diagrams was the partial integration of derivatives ∂^x_μ. For all the statements of the last Section to be valid we have to make sure that this partial integration produces no surface terms. Clearly this depends on the actual form of Δ. Contrary to other radial gauge propagators presented earlier the propagator (2.2) is well-defined at the origin (for a detailed discussion of this point c.f. [21]). Thus the behavior at the origin cannot be a source of surface terms. However things are more complicated at infinity. A careful inspection of the propagator (2.2) shows that for large x the first and third contribution decreases like $1/(x^2)^{D/2-1}$. Also the propagator for the Feynman gauge (A2) shows this rate of decrease and there no problems with surface terms appear. However the second and fourth contribution of (2.2) drops only like $1/(x^2)^{(D-3)/2}$. This weaker rate of decrease is always accompanied by a partial derivative ∂^x_μ. The worst case that might appear is that all legs at a vertex are of this type. A typical example for such a coincidence is

$$\int d^Dw \int d^Dx \int d^Dy\, T^{\lambda\mu\nu}_{abc}(w,x,y)\,\partial^w_\lambda \Delta_{\lambda'}(w,w')\partial^x_\mu \Delta_{\mu'}(x,x')\partial^y_\nu \Delta_{\nu'}(y,y')\,. \tag{4.5}$$

Inserting (A4) and evaluating the δ-functions we are left with a D dimensional integral and an integrand with a partial derivative and three $\partial\Delta$ contributions. Hence the behavior for large x is given by $\int dx/(x^2)^{D-7/2}$ which might cause a logarithmic surface term for $D \to 4$. Before discussing this case in more detail we note that this actually is the only problematic case. If any of the $\partial\Delta$ contributions is replaced by a term which falls off like $1/(x^2)^{D/2-1}$ no surface term shows up if D is in the vicinity of 4. If there is any surface term it would be caused by a partial integration in (4.5). Fortunately we can calculate this potential surface term explicitly by inserting the definition for the three gluon vertex (A4) and using (3.4). We find

$$\begin{aligned}&\int d^Dw \int d^Dx \int d^Dy\, T^{\lambda\mu\nu}_{abc}(w,x,y)\,\partial^w_\lambda \Delta_{\lambda'}(w,w')\partial^x_\mu \Delta_{\mu'}(x,x')\partial^y_\nu \Delta_{\nu'}(y,y') \\ &+ \int d^Dw \int d^Dx \int d^Dy\, \partial^w_\lambda T^{\lambda\mu\nu}_{abc}(w,x,y)\,\Delta_{\lambda'}(w,w')\partial^x_\mu \Delta_{\mu'}(x,x')\partial^y_\nu \Delta_{\nu'}(y,y') = 0\,.\end{aligned} \tag{4.6}$$

Thus also in this problematic case no surface term appears.

We conclude that for the manipulations of radial gauge Feynman diagrams partial integrations can be performed without any problems. Therefore the diagrammatic scheme presented in the last Section can be applied to the radial gauge Feynman rules. This proves that a consistent set of Feynman rules for the radial gauge is given by the radial propagator (2.2) and the usual three and four gluon vertices (A4) and (A5), respectively. The ghost fields decouple (for the temporal gauge this depends explicitly on the pole prescription) and no additional vertices are necessary (for the Coulomb gauge one has to encounter that problem).

V. SLAVNOV-TAYLOR IDENTITIES

Slavnov-Taylor identities for Yang-Mills fields formulated in radial gauge have already been derived in [16]. Besides the diagrammatic scheme presented in Sec. III these identities also serve to check the consistency of a set of Feynman rules. In addition these identities are an important ingredient to set up a renormalization scheme for radial gauge perturbation theory. For this latter aspect we refer to the remarks made in [16].

In the following we only study the consequences of the Slavnov-Taylor identities for the gluon self energy. In principle also higher one-particle irreducible n-point functions can be studied. We start with the generating functional for Yang-Mills fields in radial gauge and introduce a Lagrange multiplier field C:

$$\begin{aligned} W[J] := & \int \mathcal{D}A \; \delta(x_\mu A^\mu(x)) \\ & \times \exp\left(i \int d^D x \, (\mathcal{L}_{\rm YM}[A](x) + J^a_\mu(x) A^\mu_a(x)) \right) \\ = & \int \mathcal{D}[A,C] \, \exp\left(i \int d^D x \, (\mathcal{L}_{\rm YM}[A](x) + C^a(x) x_\mu A^\mu_a(x) + J^a_\mu(x) A^\mu_a(x)) \right) . \end{aligned} \tag{5.1}$$

In addition we introduce the generating functional for vanishing source terms,

$$W_0 := W[J=0] \, , \tag{5.2}$$

and full and free Green's functions for an arbitrary quantity ξ:

$$\langle \xi \rangle := \frac{1}{W_0} \int \mathcal{D}[A,C] \, \xi \exp(iS[A,C]) \tag{5.3}$$

and

$$\langle \xi \rangle_0 := \langle \xi \rangle \Big|_{g=0} \, , \tag{5.4}$$

respectively. Here the action S is defined as

$$S[A,C] := \int d^D x \, (\mathcal{L}_{\rm YM}[A](x) + C^a(x) x_\mu A^\mu_a(x)) \, . \tag{5.5}$$

It is well-known that the operator

$$\mathcal{O}^{\mu\nu}(x) = g^{\mu\nu}\Box_x - \partial_x^\mu \partial_x^\nu \tag{5.6}$$

which appears in the free part of $\mathcal{L}_{\mathrm{QCD}}$ is not invertible due to the gauge invariance of the theory. However in the enlarged space of A and C fields the operator $\mathcal{O}$ can be inverted. We denote propagator and self energy in the larger space with

$$\begin{aligned}\bar{D}^{ab}_{\Theta\Phi}(x,y) &:= \begin{pmatrix} \langle A^a_\mu(x)\, A^b_\nu(y)\rangle & \langle A^a_\mu(x)\, C^b(y)\rangle \\ \langle C^a(x)\, A^b_\nu(y)\rangle & \langle C^a(x)\, C^b(y)\rangle \end{pmatrix} \\ &= \begin{pmatrix} D^{ab}_{\mu\nu}(x,y) & \langle A^a_\mu(x)\, C^b(y)\rangle \\ \langle C^a(x)\, A^b_\nu(y)\rangle & \langle C^a(x)\, C^b(y)\rangle \end{pmatrix}\end{aligned} \tag{5.7}$$

and $\bar{\Pi}^{ab}_{\Theta\Phi}(x,y)$, respectively. The large Greek letters denote numbers from 0 to 4. For 0 to 3 they coincide with the Lorentz indices of the gauge fields while 4 denotes the additional Lagrange multiplier field C.

The Dyson-Schwinger equation turns out to be

$$\bar{D} = \bar{D}_0 + \bar{D}_0 \bar{\Pi} \bar{D}\,, \tag{5.8}$$

where "multiplication" includes summation over all indices and integration over the space time variables, i.e. $\bar{\Pi}\bar{D}$ is an abbreviation for

$$\sum_{\Xi=0}^{4} \sum_{b=1}^{N^2-1} \int d^D x\, \bar{\Pi}^{ab}_{\Theta\Xi}(w,x)\, \bar{D}^{\Xi\Phi}_{bc}(x,y)\,. \tag{5.9}$$

$\bar{D}_0$ is the free contribution of $\bar{D}$. The inverse is the operator which appears in the free action (cf. (5.6)):

$$\left(\bar{D}_0^{-1}\right)^{ab}_{\Theta\Phi}(x,y) = -i\delta^{ab} \begin{pmatrix} \mathcal{O}_{\mu\nu}(x) & x_\mu \\ x_\nu & 0 \end{pmatrix} \delta(x-y)\,. \tag{5.10}$$

The Dyson-Schwinger equation (5.8) can be transformed to

$$\bar{\Pi} = \bar{D}_0^{-1}\,(\bar{D} - \bar{D}_0)\bar{D}^{-1}\,, \tag{5.11}$$

which can be further evaluated using the Slavnov-Taylor identities

$$\langle A^a_\mu(x)\, C^b(y)\rangle = \langle A^a_\mu(x)\, C^b(y)\rangle_0 \tag{5.12}$$

and

$$\langle C^a(x)\, C^b(y)\rangle = 0 \tag{5.13}$$

stated in [16]. We find

$$\bar{D} - \bar{D}_0 = \begin{pmatrix} D - D_0 & 0 \\ 0 & 0 \end{pmatrix}; \tag{5.14}$$

hence:

$$\begin{aligned}\bar{\Pi} &= -i \begin{pmatrix} \mathcal{O} & x \\ x & 0 \end{pmatrix} \begin{pmatrix} D - D_0 & 0 \\ 0 & 0 \end{pmatrix} \bar{D}^{-1} \\ &= -i \begin{pmatrix} \mathcal{O}(D - D_0) & 0 \\ x(D - D_0) & 0 \end{pmatrix} \bar{D}^{-1} = -i \begin{pmatrix} \mathcal{O}(D - D_0) & 0 \\ 0 & 0 \end{pmatrix} \bar{D}^{-1} \\ &= -i \begin{pmatrix} * & * \\ 0 & 0 \end{pmatrix} . \end{aligned} \tag{5.15}$$

where we have used the gauge condition (1.1) in the second line. Stars denote arbitrary values. Since the self energy is symmetric with respect to an exchange of all variables we conclude that it has a non-vanishing contribution in the gauge sector, only:

$$\bar{\Pi} = \begin{pmatrix} \Pi & 0 \\ 0 & 0 \end{pmatrix} . \tag{5.16}$$

In addition we get the transversality of the self energy by multiplying (5.15) with $(\partial_\mu, 0)$ from the left

$$(\partial\Pi, 0) = (\partial, 0)(-i) \begin{pmatrix} \mathcal{O}(D - D_0) & 0 \\ 0 & 0 \end{pmatrix} \bar{D}^{-1} = (0, 0) , \tag{5.17}$$

due to $\partial\mathcal{O} = 0$ (cf. (5.6)).

We conclude that as a consequence of the Slavnov-Taylor identities the radial gauge gluon self energy obeys the transversality condition

$$\partial^x_\mu \Pi^{\mu\nu}(x, y) = 0 \tag{5.18}$$

We will finish this Section by checking this equation for the lowest order contribution in the coupling constant. Fortunately we can use the diagrammatic rules of Sec. III. Since the ghost fields decouple only two diagrams contribute to the self energy at order g^2. They are shown in Fig. 14. To derive the r.h.s. we have made use of the fact that the first diagram of Fig. 14 is symmetric with respect to an exchange of upper and lower line. In addition we have applied the diagrammatic rule of Fig. 2. Using the relation shown in Fig. 13 we find that the last diagram in Fig. 14 is exactly canceled by the last but one diagram. The remaining diagram involving G vanishes since G is contracted with a radial propagator D, i.e.

$$\int d^D y \, G^{abc}_\nu(x, y) \, D^{\nu\nu'}_{cc'}(y, y') \sim y_\nu D^{\nu\lambda}_{cc'}(y, y') = 0 . \tag{5.19}$$

This proves that the g^2 contribution to the gluon self energy indeed satisfies (5.18). Again this demonstrates the consistency of our set of radial gauge Feynman rules as well as the usefulness of the diagrammatic rules presented in Sec. III.

VI. CONCLUSIONS

In this article we have presented a complete set of radial gauge Feynman rules for non-Abelian gauge fields. The rather surprising results concerning the radial gauge field propagator have already been discussed in [21]:

- The propagator can be expressed in terms of a gauge invariant Wilson loop;
- it is singular in four dimensional space;
- this singularity is necessary to reproduce correct results for gauge invariant quantities.

The other properties of this set of rules are:

- Feynman rules must be formulated in coordinate space since the gauge condition explicitly breaks translational invariance;
- ghost fields decouple;
- besides the conventional three and four gluon vertices no additional vertices are necessary.

Introducing such a new set of rules it is crucial to show its consistency with the conventional covariant gauge Feynman rules, i.e. to prove that results for gauge invariant quantities calculated with both sets of rules agree with each other. To achieve that we have generalized the theorem of equivalence to coordinate space Feynman rules. Originally it was developed by Cheng and Tsai to check the consistency of different sets of Feynman rules formulated in momentum space.

To the best of our knowledge such a systematic study of coordinate space Feynman rules has never been presented before. In [20] the consistency of radial gauge Feynman rules was checked by an explicit one loop calculation using basically the same technique as presented here. However it was not pointed out there how this technique could be generalized to other Feynman diagrams involving higher order loops. In addition the radial gauge propagator used in [20] was later shown to be incorrect [17].

A few additional remarks concerning the singularity of the radial gauge propagator (2.2) are necessary: In principle there are three sources for a possible singular behaviour. First, the already mentioned cusp singularity discussed in great detail in [21]. Second, an additional singularity shows up if x and y are aligned with respect to the origin. These divergences are already present in Euclidean space. In Minkowski space a third type of singularity appears if $x - y$ is light-like. Of course it would be interesting to study also the latter two types of singularities in more detail. At least the third one is also connected to Wilson loops with part of the contour on the light cone [26]. Despite the lack of a more detailed examination of these additional singularities we note that all these singularities are regularized by dimensional regularization. Thus also these divergences do not spoil the arguments presented in this article.

To set up perturbation theory in radial gauge a complete set of Feynman rules is of course only the first step. Next one must figure out how renormalization works in this gauge. Due to the lack of translational invariance one might suspect that local counter terms are insufficient to renormalize the theory. However some arguments that this is not the case are given in [16]. Further general considerations as well as explicit loop calculations of self energies and vertex corrections are necessary to work out a renormalization scheme for radial gauge. We expect that the diagrammatic scheme presented here might serve to simplify such calculations.

ACKNOWLEDGMENTS

I thank Ulrich Heinz for stimulating discussions and support. I also acknowledge useful discussions with Heribert Weigert and Marc Achhammer. This research was supported in part by Deutsche Forschungsgemeinschaft and Bundesministerium für Bildung, Wissenschaft, Forschung und Technologie.

APPENDIX A: FEYNMAN RULES IN COORDINATE SPACE

Since Feynman rules are commonly used in momentum space we have collected some coordinate space expressions for propagators and vertices in this Appendix.

In Minkowski space with one time and $D-1$ space dimensions the propagator of a scalar particle is given by [27]

$$\begin{aligned}\Delta_S(x-y) &= \int \frac{d^Dk}{(2\pi)^D}\,\frac{-i}{k^2+i\eta}\,e^{-ik\cdot(x-y)} \\ &= \frac{\Gamma(D/2-1)}{4\pi^{D/2}}\,[(x-y)^2-i\epsilon]^{1-D/2} \quad , \quad \eta,\epsilon\to+0\,. \end{aligned} \tag{A1}$$

The Feynman propagator got additional factors of unity in Lorentz and color space

$$\langle B^a_\mu(x) B^b_\nu(y)\rangle_{\rm Feyn} = \delta^{ab}\,D^F_{\mu\nu}(x,y) = \delta^{ab}\,g_{\mu\nu}\,\Delta_S(x-y)\,. \tag{A2}$$

We define the (full) three gluon vertex $\mathbf{T}$ as

$$\begin{aligned}&\langle A^a_\lambda(w)\,A^b_\mu(x)\,A^c_\nu(y)\rangle = \\ &\int d^Dw'\,d^Dx'\,d^Dy'\,\langle A^a_\lambda(w)\,A^{a'}_{\lambda'}(w')\rangle\langle A^b_\mu(x)\,A^{b'}_{\mu'}(x')\rangle\langle A^c_\nu(y)\,A^{c'}_{\nu'}(y')\rangle \mathbf{T}^{\lambda'\mu'\nu'}_{a'b'c'}(w',x',y')\,;\end{aligned} \tag{A3}$$

the four gluon vertex $\mathbf{Q}$ is defined in a completely analogous way.

The expressions in lowest order of the coupling constant (bare vertices) are given by

$$\begin{aligned}T^{\lambda\mu\nu}_{abc}(w,x,y) = -igf_{abc}\Big[&g^{\lambda\mu}(\partial^\nu_w-\partial^\nu_x)\,\delta(x-y)\,\delta(w-y) \\ &+ g^{\mu\nu}(\partial^\lambda_x-\partial^\lambda_y)\,\delta(y-w)\,\delta(x-w) \\ &+ g^{\nu\lambda}(\partial^\mu_y-\partial^\mu_w)\,\delta(w-x)\,\delta(y-x)\Big]\end{aligned} \tag{A4}$$

and

$$\begin{aligned}Q^{\kappa\lambda\mu\nu}_{abcd}(v,w,x,y) = -ig^2\Big[&f_{abe}f_{cde}(g^{\kappa\mu}g^{\nu\lambda}-g^{\kappa\nu}g^{\lambda\mu}) \\ &+ f_{ace}f_{dbe}(g^{\kappa\nu}g^{\lambda\mu}-g^{\kappa\lambda}g^{\mu\nu}) \\ &+f_{ade}f_{bce}(g^{\kappa\lambda}g^{\mu\nu}-g^{\kappa\mu}g^{\nu\lambda})\Big]\,\delta(v-w)\,\delta(v-x)\,\delta(v-y)\,.\end{aligned} \tag{A5}$$

APPENDIX B: ADDITIONAL GRAPHICAL RULES

Here we complete the set of diagrammatic rules presented in Sec. III. In addition to Fig. 2, 7, 9, and 13 we have to discuss the case that a contraction arrow points at a four gluon vertex (Fig. 15) or at a ghost gluon vertex (Fig. 16). The corresponding formulae are

$$\begin{aligned}
&\int d^D v'\, g f_{eah} g^{\kappa}{}_{\kappa'} \delta(u-v)\,\delta(u-v')\, Q^{\kappa'\lambda\mu\nu}_{hbcd}(v',w,x,y) \\
&\quad + \int d^D w'\, g f_{ebh} g^{\lambda}{}_{\lambda'} \delta(u-w)\,\delta(u-w')\, Q^{\kappa\lambda'\mu\nu}_{ahcd}(v,w',x,y) \\
&= \int d^D x'\, g f_{ehc} g^{\mu}{}_{\mu'} \delta(u-x)\,\delta(u-x')\, Q^{\kappa\lambda\mu'\nu}_{abhd}(v,w,x',y) \\
&\quad + \int d^D y'\, g f_{ehd} g^{\nu}{}_{\nu'} \delta(u-y)\,\delta(u-y')\, Q^{\kappa\lambda\mu\nu'}_{abch}(v,w,x,y')
\end{aligned} \tag{B1}$$

for Fig. 15 and

$$\begin{aligned}
&\int d^D v'\, G^{abe}_{\mu}(w,v')\,\delta(v-v')\, g f^{ecd} \delta(x-v')\,\delta(x-y) = \\
&\int d^D v'\, G^{dbe}_{\nu}(w,v')\,\delta(y-v')\, g f^{eca} g^{\nu}{}_{\mu} \delta(x-v)\,\delta(x-v') \\
&+ \int d^D v'\, G^{ebc}_{\nu}(w,x)\,\delta(v'-x)\, g f^{eda} g^{\nu}{}_{\mu} \delta(y-v)\,\delta(y-v')\,.
\end{aligned} \tag{B2}$$

for Fig. 16. The last relation is a somewhat complicated way to write down the Bianchi identity for the structure constants.[4] It is missing in [6].

For Wilson loops we have to encounter the case that a partial derivative (arrow) "meets" a contour integral, e.g.

$$\begin{aligned}
&\int\limits_0^1 d\sigma_1 \int\limits_0^1 d\sigma_2 \int\limits_0^1 d\sigma_3\, \Theta(\sigma_1>\sigma_2>\sigma_3)\, \dot w_{\mu_1}(\sigma_1)\, \dot w_{\mu_2}(\sigma_2)\, \dot w_{\mu_3}(\sigma_3) \\
&\quad \times \int d^D x_1 \int d^D x_2 \int d^D x_3\, D^{\mu_1\nu_1}(w(\sigma_1),x_1) \partial^{\mu_2}_{w(\sigma_2)}\, \Delta^{\nu_2}(w(\sigma_2),x_2) D^{\mu_3\nu_3}(w(\sigma_3),x_3) \\
&\quad \times T^{a_1a_2a_3}_{\nu_1\nu_2\nu_3}(x_1,x_2,x_3)\, \mathrm{Sp}(t_{a_1}t_{a_2}t_{a_3}) \\
&= \int\limits_0^1 d\sigma_1 \int\limits_0^{\sigma_1} d\sigma_3 \int\limits_{\sigma_3}^{\sigma_1} d\sigma_2\, \dot w_{\mu_1}(\sigma_1)\, \dot w_{\mu_2}(\sigma_2)\, \dot w_{\mu_3}(\sigma_3) \\
&\quad \times \int d^D x_1 \int d^D x_2 \int d^D x_3\, D^{\mu_1\nu_1}(w(\sigma_1),x_1) \partial^{\mu_2}_{w(\sigma_2)}\, \Delta^{\nu_2}(w(\sigma_2),x_2) D^{\mu_3\nu_3}(w(\sigma_3),x_3) \\
&\quad \times T^{a_1a_2a_3}_{\nu_1\nu_2\nu_3}(x_1,x_2,x_3)\, \mathrm{Sp}(t_{a_1}t_{a_2}t_{a_3})\,.
\end{aligned} \tag{B3}$$

Here $w(\sigma)$, $\sigma\in[0,1]$, parameterizes an arbitrary Wilson loop contour. We make use of the relation

$$\dot w_{\mu_2} \partial^{\mu_2}_{w(\sigma_2)} = \frac{d}{d\sigma_2} \tag{B4}$$

---

[4] $f^{abe}f^{cde} + f^{ace}f^{dbe} + f^{ade}f^{bce} = 0$.

to evaluate the contour integral:

$$\int_0^1 d\sigma_1 \int_0^{\sigma_1} d\sigma_3\, \dot{w}_{\mu_1}(\sigma_1)\, \dot{w}_{\mu_3}(\sigma_3) \int d^D x_1 \int d^D x_2 \int d^D x_3\, D^{\mu_1\nu_1}(w(\sigma_1), x_1)$$
$$\times \left[\Delta^{\nu_2}(w(\sigma_1), x_2) - \Delta^{\nu_2}(w(\sigma_3), x_2)\right] D^{\mu_3\nu_3}(w(\sigma_3), x_3)$$
$$\times T^{a_1 a_2 a_3}_{\nu_1\nu_2\nu_3}(x_1, x_2, x_3)\, \mathrm{Sp}(t_{a_1} t_{a_2} t_{a_3})\,. \tag{B5}$$

This is depicted in Fig. 17. In addition it is shown how the result is related to other diagrams [11].

REFERENCES

[1] P. Pascual and R. Tarrach, *QCD: Renormalization for the Practitioner*, Lecture Notes in Physics, Vol. 194 (Springer, Berlin, 1984).

[2] S. Caracciolo, G. Curci, and P. Menotti, Phys. Lett. **B113** (1982) 311.

[3] P.V. Landshoff, in: *Physical and Nonstandard Gauges*, Lecture Notes in Physics, Vol. 361 (Springer, Berlin, 1990), 74ff.

[4] J.-P. Leroy, J. Micheli, and G.-C. Rossi, Z. Phys. **C36** (1987) 305.

[5] F. Palumbo, Phys. Lett. **B243** (1990) 109.

[6] H. Cheng and E.-C. Tsai, *The Theorem of Equivalence and The Anomalous Coulomb Interaction*, MIT-preprint (1986).

[7] H. Cheng and E.-C. Tsai, Phys. Rev. Lett. **57** (1986) 511.

[8] P. Doust, Ann. Phys. **177** (1987) 169.

[9] P. J. Doust and J.C. Taylor, Phys. Lett. **B197** (1987) 232.

[10] N. H. Christ and T. D. Lee, Phys. Rev. **D22** (1980) 939.

[11] H. Cheng and E.-C. Tsai, Phys. Rev. **D36** (1987) 3196.

[12] V. A. Fock, Sov. Phys. **12** (1937) 404.

[13] J. Schwinger, Phys. Rev. **82** (1952) 684.

[14] C. Cronström, Phys. Lett. **B90** (1980) 267.

[15] M. A. Shifman, Nucl. Phys. **B173** (1980) 13.

[16] W. Kummer and J. Weiser, Z. Phys. **C31** (1986) 105.

[17] G. Modanese, J. Math. Phys. **33** (1992) 1523.

[18] P. Menotti, G. Modanese, and D. Seminara, Ann. Phys. **224** (1993) 110.

[19] P. Menotti and D. Seminara, Nuovo Cim. **106A** (1993) 187.

[20] R. Delbourgo and Triyanta, Int. J. Mod. Phys. **A7** (1992) 5833.

[21] S. Leupold and H. Weigert, eprint hep-th/9604015, to appear in Phys. Rev. D.

[22] R. A. Brandt, F. Neri, and M.-A. Sato, Phys. Rev. **D24** (1981) 879.

[23] M. Achhammer, U. Heinz, S. Leupold, and U.A. Wiedemann, *Gauge Invariance of Resummation Schemes: The QCD Partition Function*, in preparation.

[24] Y.J. Feng and C.S. Lam, Phys. Rev. **D53** (1996) 2115.

[25] Y.J. Feng and C.S. Lam, eprint hep-ph/9608219.

[26] I. A. Korchemskaya and G. P. Korchemsky, Phys. Lett. **B287** (1992) 169.

[27] T.-P. Cheng and L.-F. Li, *Gauge theory of elementary particle physics* (Oxford University Press, Oxford, 1988) 219f.

FIGURES

FIG. 17. Additional relation for Wilson loops.

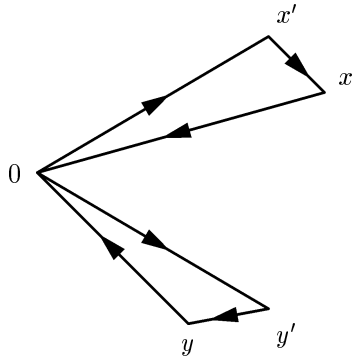

FIG. 1

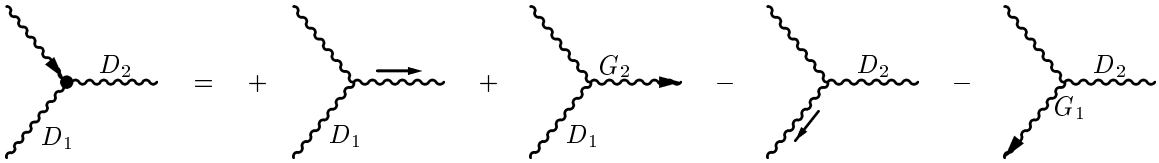

FIG. 2

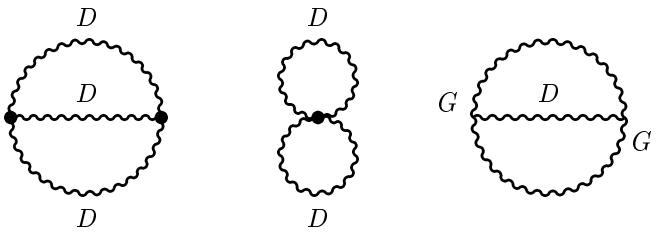

FIG. 3

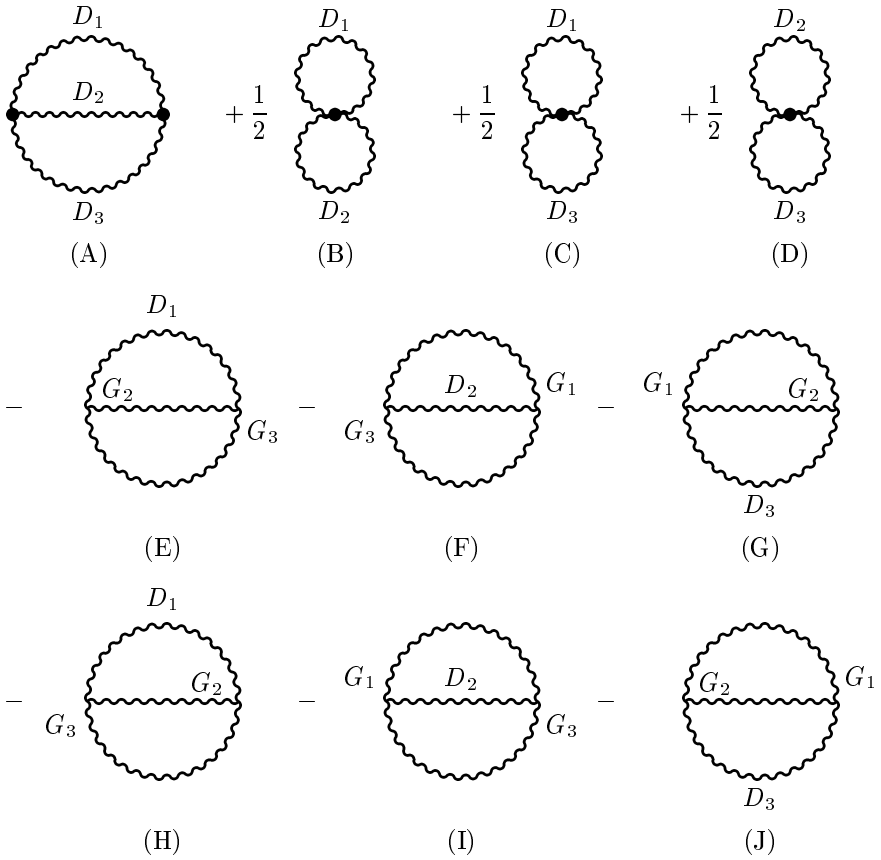

FIG. 4

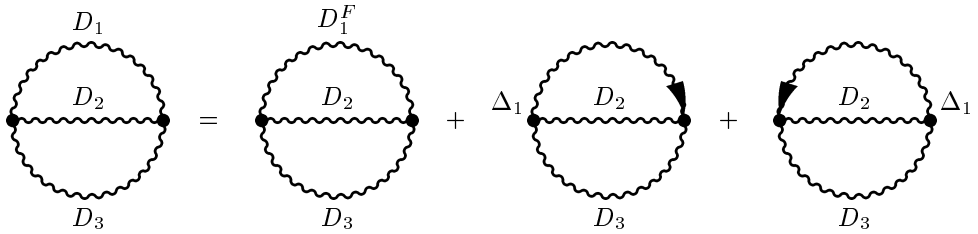
D_1
D_2
D_3
=
D_1^F
D_2
D_3
+
Δ_1
D_2
D_3
+
D_2
Δ_1
D_3

FIG. 5

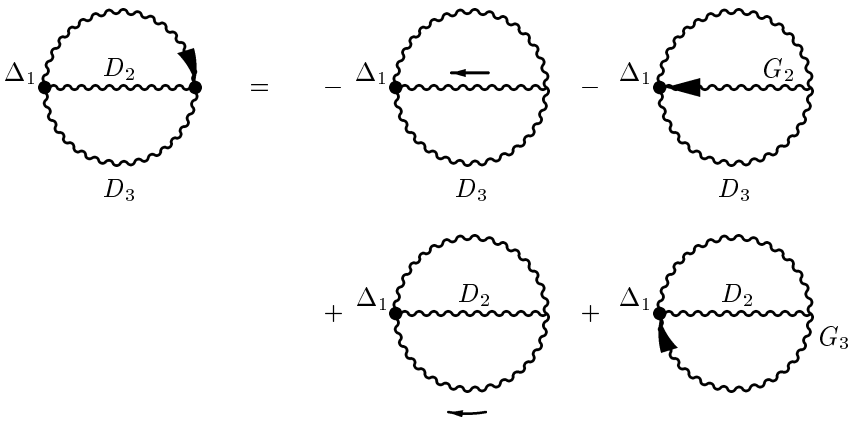
Δ_1
D_2
D_3
=
−
Δ_1
D_3
−
Δ_1
G_2
D_3
+
Δ_1
D_2
+
Δ_1
D_2
G_3

FIG. 6

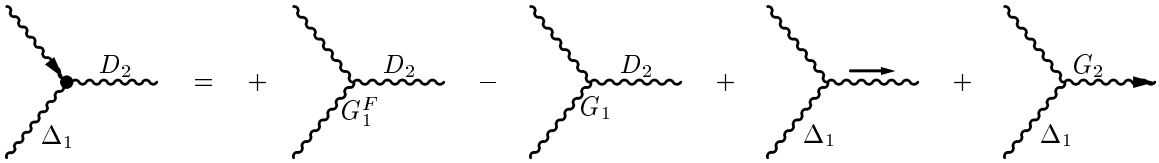
D_2
Δ_1
=
+
D_2
G_1^F
−
D_2
G_1
+
Δ_1
+
G_2
Δ_1

FIG. 7

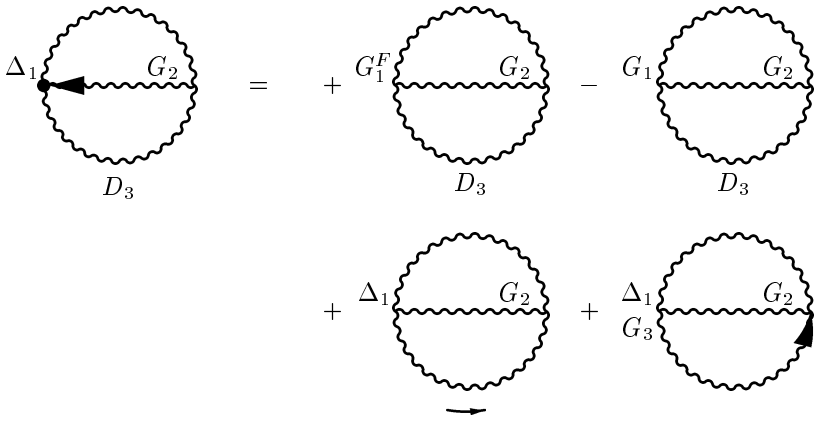
Δ_1
G_2
D_3
=
+
G_1^F
G_2
D_3
−
G_1
G_2
D_3
+
Δ_1
G_2
+
Δ_1
G_3
G_2

FIG. 8

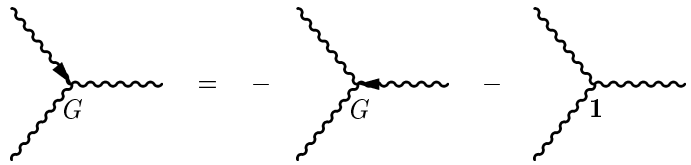

FIG. 9

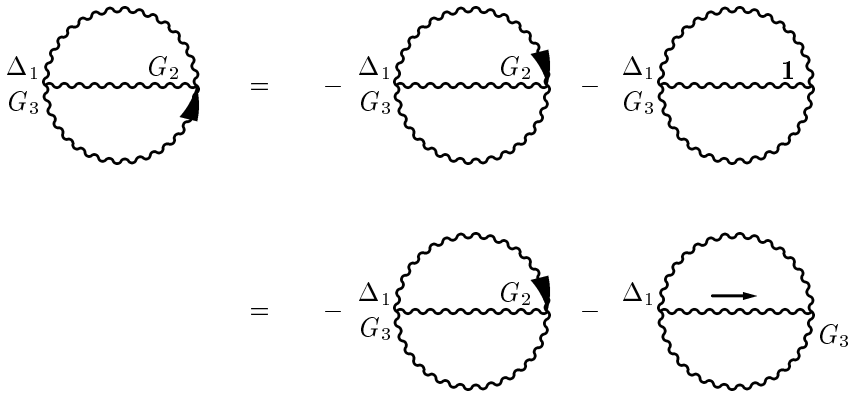

FIG. 10

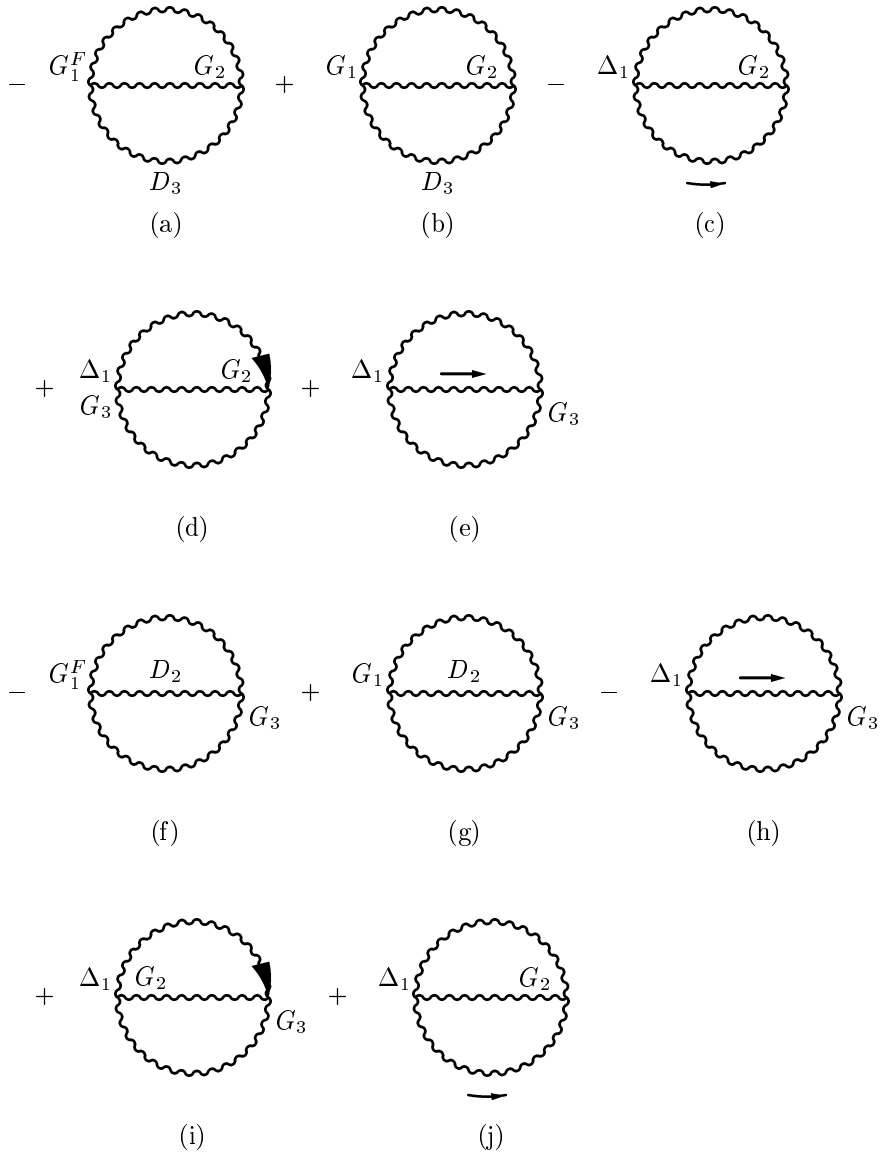
$-$
G_1^F
G_2
D_3
(a)
$+$
G_1
G_2
D_3
(b)
$-$
Δ_1
G_2
(c)
$+$
Δ_1
G_2
G_3
(d)
$+$
Δ_1
G_3
(e)
$-$
G_1^F
D_2
G_3
(f)
$+$
G_1
D_2
G_3
(g)
$-$
Δ_1
G_3
(h)
$+$
Δ_1
G_2
G_3
(i)
$+$
Δ_1
G_2
(j)

FIG. 11

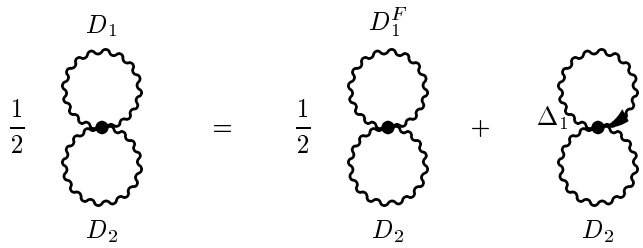

FIG. 12

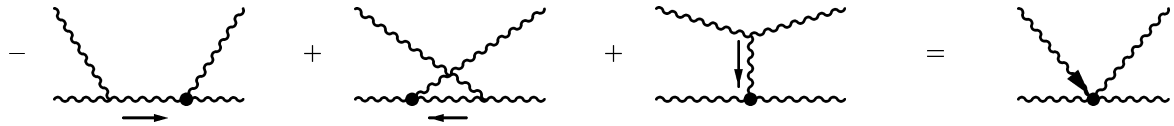

FIG. 13

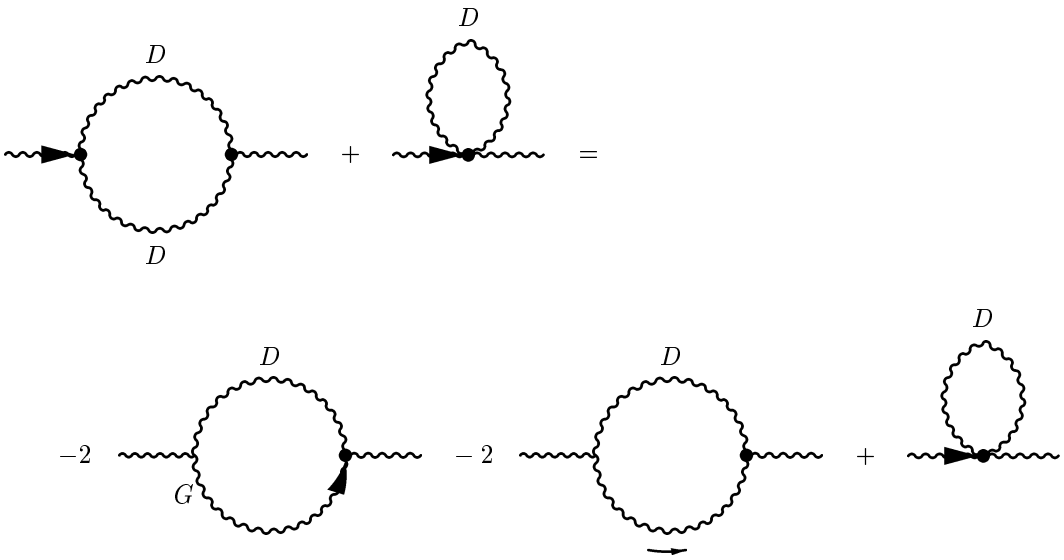

FIG. 14

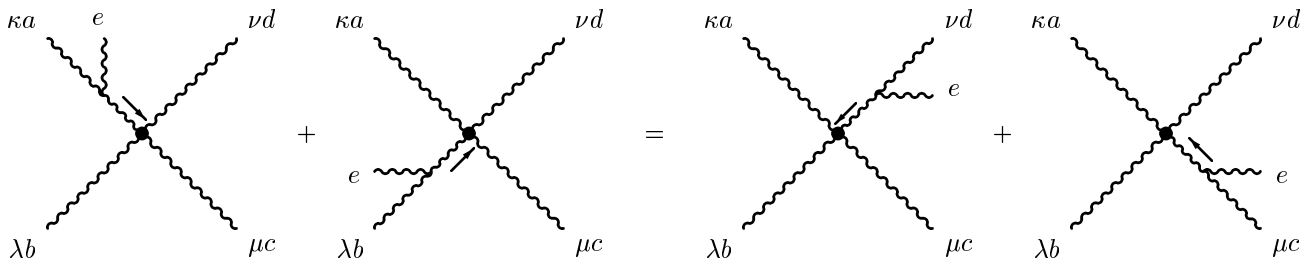

FIG. 15

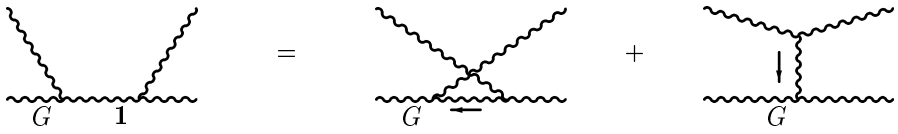

FIG. 16

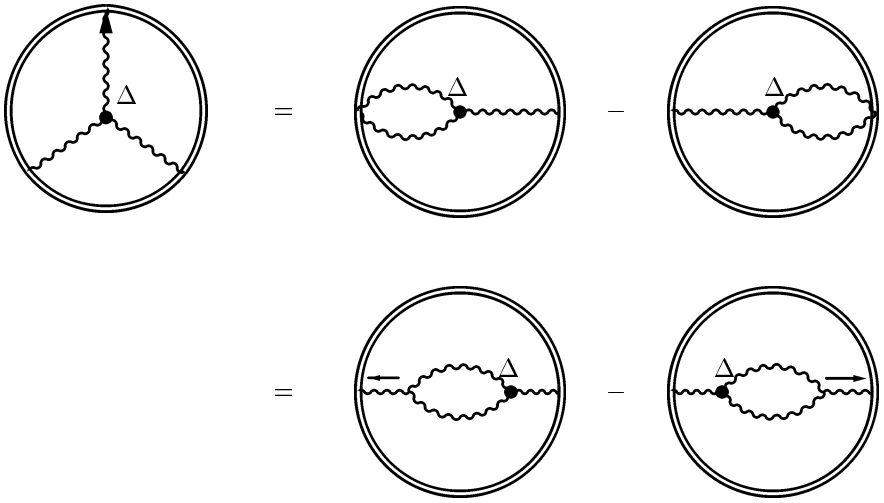

FIG. 17